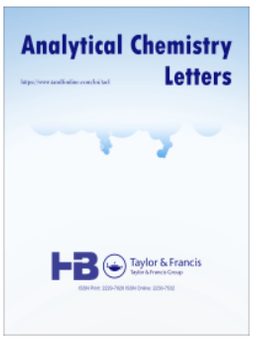

Analytical Chemistry Letters

ISSN: (Print) (Online) Journal homepage: https://www.tandfonline.com/loi/tacl20

Structure Based Design of Tubulin Binding 9-Arylimino Noscapinoids: Chemical Synthesis and Experimental Validation Against Breast Cancer Cell Lines

Pratyush Pragyandipta, Rajesh Kumar Meher, Praveen Kumar Reddy, Ravikumar Pedaparti, Srinivas Kantevari & Pradeep K. Naik

To cite this article: Pratyush Pragyandipta, Rajesh Kumar Meher, Praveen Kumar Reddy, Ravikumar Pedaparti, Srinivas Kantevari & Pradeep K. Naik (2022) Structure Based Design of Tubulin Binding 9-Arylimino Noscapinoids: Chemical Synthesis and Experimental Validation Against Breast Cancer Cell Lines, Analytical Chemistry Letters, 12:1, 29-43, DOI: 10.1080/22297928.2021.2009029

To link to this article: https://doi.org/10.1080/22297928.2021.2009029

Analytical Chemistry Letters
https://www.tandfonline.com/loi/tacl

Taylor & Francis
Taylor & Francis Group

ISSN: 2229-7928 (Print); ISSN: 2230-7532 (Online)

Article

Structure Based Design of Tubulin Binding 9-Arylimino Noscapinoids: Chemical Synthesis and Experimental Validation Against Breast Cancer Cell Lines

Pratyush Pragyandipta [1], Rajesh Kumar Meher [1], Praveen Kumar Reddy [2], Ravikumar Pedaparti [2], Srinivas Kantevari [2] and Pradeep K. Naik [1]*

[1] Centre of Excellence in Natural Products and Therapeutics, Department of Biotechnology and Bioinformatics, Sambalpur University, Jyoti Vihar, Burla, Sambalpur-768019, Odisha, India

[2] Fluoro and Agrochemicals Division, CSIR-Indian Institute of Chemical Technology, Hyderabad 500007, India

* *Corresponding Author: pknaik1973@suniv.ac.in (Pradeep K. Naik)*

Received 29 August 2021; Received in revised form 15 November 2021; Accepted 16 November 2021Volorumq

Abstract: A novel class of noscapine derivatives known as 9-arylimino noscapinoids was designed by substituting arylimino groups (Schiff bases) at the C-9 position. These molecules were docked with αβ-tubulin complex and a panel of three top scoring molecules, 4-6 based on docking score were screened out. These molecules bind tubulin with robust predicted binding energy of -37.24 kcal/mol and -45.41 kcal/mol for 4, -39.73 kcal/mol and -47.74 kcal/mol for 5, and -43.62 kcal/mol and -49.72 kcal/mol for 6 respectively compared to noscapine (-34.47 kcal/mol and -40.27 kcal/mol) using molecular mechanics/Poisson-Boltzmann surface area (MM/PBSA) and molecular mechanics/generalized Born surface area (MM/GBSA). These three molecules were chemically synthesized and demonstrated experimentally to bind tubulin with high affinity compared to noscapine. The anti-proliferative activity of 4-6 revealed inhibitory concentration (IC_{50} value) in between 3.6 to 32.6 μM using MCF-7 and MDA-MB-231 human breast cancer cell lines and a group of primary breast tumor cells. All three molecules were shown to inhibit the mitotic progression at the G2/M phase and induce apoptosis to cancer cells at a different level. Thus, we conclude that 9-arylimino noscapinoids 4-6 have tremendous potential as chemotherapeutic agents for the treatment of breast cancer.

Keywords: 9-arylimino noscapinoids; Anticancer agents; Breast cancer; Molecular docking; Noscapine; Tubulin targeting.

Introduction

Microtubule-interacting drugs, for example, taxols and vinca alkaloids have been used in the clinic for the treatment of various malignancies. However, these drugs are known to cause severe dose-dependent toxicities in patients such as peripheral neuropathy, systemic toxicity, and allergic reactions [1,2]. More importantly, patients are developing resistance against taxol. Thus, the wonderful promise of taxol in managing breast cancers justifies further efforts to discover novel mitotic inhibitors. Better yet, it would be additionally useful if other novel anti-mitotic agents have fewer side effects and are easily administered. In a quest of finding such compounds, the natural compounds were screened and noscapine (an opium alkaloid that is in the clinic as a safe anti-tussive drug)

DOI: 10.1080/22297928.2021.2009029

was discovered [3]. It was shown to bind tubulin, without interfering with the tubulin organization (monomer/polymer ratio) [4]. It was found to kill cancer cells of different tissue origins, including those that are resistant to conventional chemotherapeutics. It doesn't show any severe side effects among volunteers [5]. It was found to regress the volume of the implanted tumor to a fair degree in xenograft breast cancer animal models at a high dosage of 600 mg/kg.

From an ongoing quest to improve our therapeutic arsenal, we have developed a battery of derivatives by modification of its scaffolds and demonstrated to have high tubulin binding and anti-tumor activity compared to noscapine without any debilitating toxicities [6-8]. While several synthesized derivatives of noscapinoids showed promising *in vitro* activity against breast tumor cell lines, the antiproliferative activity comes to be in higher concentration. Therefore, there is an urgent need to take up further optimization of noscapine towards the development of novel and more promising derivatives.

In a quest of developing new derivatives with better anticancer activity, we appeal to developing 9-arylimino congeners of noscapine by substituting arylimino groups at the C-9 position of the noscapine scaffold. The promising analogues were then chemically synthesized and their anticancer activity was evaluated using two human breast cancer cell lines (MCF-7 and MDA-MB-231). The 9-arylimino derivatives of noscapine were found to bind tubulin heterodimer with enhanced binding affinity, efficiently suppress cancer cell growth, successfully trigger cancer cell apoptosis by the arrest of cancer cells at the G2/M phase.

Materials and methods

Refinement of the crystal structure of tubulin

The co-complex structure of tubulin-amino noscapine was downloaded from the PDB data bank (PDB ID: 6Y6D). This structure of tubulin was obtained at a higher resolution of 2.20 Å through X-ray crystallography [9]. The structure was visualized using Maestro (Schrodinger software package) and the tubulin heterodimer consisting of α- and β- tubulin was prepared based on the multistep procedure of the protein preparation wizard (Schrodinger software package).

Design of 9-arylimino congeners of noscapine

Based on *in silico* combinatorial approach 9-arylimino congeners of noscapine were designed by hybridizing with arylimino groups (Schiff bases) as depicted in Fig. 1 and a library of 17 compounds was developed (supplementary information S1). It was reported previously that Schiff base analogs have impressive anticancer activity. As an example, Schiff bases from coumarin and pyrazole aldehyde have been tested against cancer cell lines that showed mild anticancer activities [10]. Furthermore, mono and bis-Schiff bases have been reported efficacious against five cancer cell lines [11].

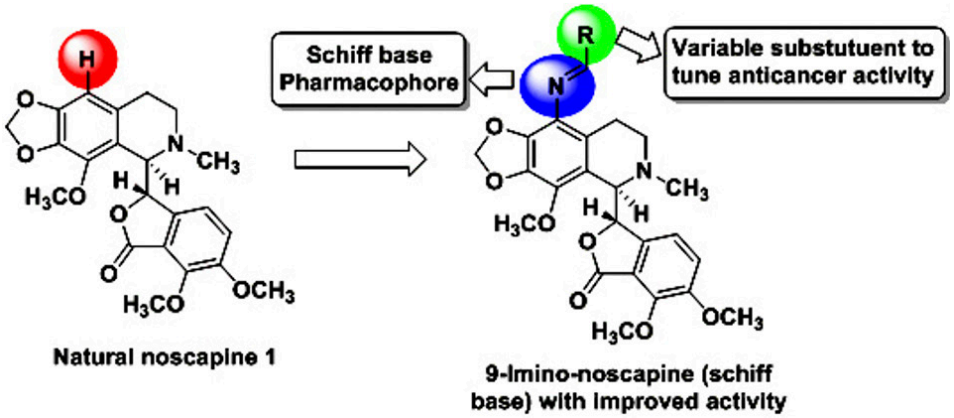

Figure 1. Strategic development of 9-arylimino noscapinoids by hybridizing Schiff base at C-9 position of the isoquinoline ring system of noscapine

Preparation of ligands and optimization

We have built the molecular structures of 9-arylimino derivatives of noscapine (Fig. 1) using ISIS draw and converted them into 3D structures using Chemsketch. Macromodel (Schrodinger software package and OPLS 2005 force field was used for energy minimization of build structures using PRCG algorithm. A simulation of 1000 steps and an energy gradient of 0.001 were used for energy minimization. The molecules were also geometrically refined using Jaguar (version 17.4, Schrödinger, LLC) with a basis set of 3-21G* [12] using Becke's three-parameter exchange potential and the Lee-Yang-Parr correlation functional (B3LYP) [13]. Ligprep (Schrödinger software package) was used to generate ionization states at physiological pH, generation of possible tautomers, and minimization of the ring conformations for each molecule.

Molecular docking

The docking protocol used was validated by the superimposition of the crystal structure of amino-noscapine with its docked structure and calculating the root mean square deviation (RMSD) between them. The RMSD value of 0.806 between crystal structure and docked structure validated the docking protocol. After validating the docking protocol the library of 9-arylimino derivatives of noscapine designed above was docked onto the noscapinoids binding site [9] located at α- and β- tubulin interface. The noscapinoids binding site was selected based on the co-crystal structure of tubulin and one of the derivatives of noscapine "amino-noscapine" (PDB ID: 6Y6D) [9]. Further, the binding site was specified by generating two grid boxes as described earlier [14] by selecting the co-crystal ligand, amino-noscapine using the Glide Grid generation programme. The molecules were docked using Glide-XP algorithm [15] (Schrodinger software package) and evaluated using Glide XP_{Score} function [15] with similar parameters set up as mentioned earlier [14]. All the molecules in the library were sorted based on their docking score (supplementary information S2) and finally the best three molecules 4-6 (Fig. 2) based on their docking score were selected for chemical synthesis and experimental evaluation to confirm their anticancer potential.

Molecular dynamics simulations

The docked complexes of tubulin and 9-arylimino noscapinoids, 4-6 in the presence of GTP, GDP and magnesium were used for molecular dynamics simulation using GROMACS 2019.2 package. The parameter files for tubulin and the ligands were generated as mentioned earlier [16]. Topologies for ligands were generated using tleap program of Amber18 and ACPYPE software. TIP3P water model with dissolved counter ions were added to neutralize the system. The energy minimization and molecular dynamic simulation of the system for 100 ns with a time step of 2 fs were performed with the similar parameters

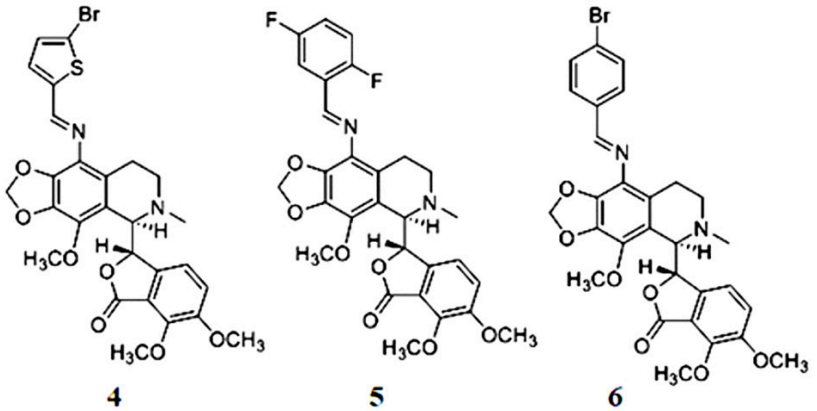

Figure 2. Molecular structure of three top ranked 9-arylimino noscapinoids, 4-6 screened out from the library based on the docking score

set up as mentioned earlier [14]. Gromacs tools were used to analyze trajectories for root mean square deviation (RMSD) and root mean square fluctuation (RMSF). All plots were generated using GRACE software.

Prediction of binding free energy using MM-PBSA and MM-GBSA technique

The MM/PBSA and MM/GBSA methods [17,18] were used for predicting the binding free energy ($\Delta G_{bind,pred}$) of 9-arylimino noscapinoids, 4-6 with tubulin using AMBER 16.0. We have used both approaches because many studies have compared the accuracy of MM/PBSA and MM/GBSA, indicating better results for MM/PBSA [19,20]. It was also found that MM/PBSA results are worse [21] or equally good [22] compared to MM/GBSA depending on the studied systems. From the last 10 ns of the MD trajectory, 500 snapshots of the structure were collected at an interval of 20 ps to determine $\Delta G_{bind,pred}$ of the molecules.

General procedure for chemical synthesis of 9-arylimino noscapinoids, 4-6

Amino-noscapine 3 was synthesized from the natural α-noscapine as reported earlier [8]. Form the amino-noscapine, the selected 9-arylimino noscapinoids 4-6 were synthesized as per the synthetic scheme (Fig. 3) as mentioned earlier [16]. Structural elucidation of intermediates and final products 4-6 were performed using NMR (^{1}H and ^{13}C), IR spectroscopy and mass (HRMS) spectrometry techniques (Supplementary information S3-S13). The final products were purified through HPLC using C18 column (acetonitrile: water, 90:10) and were >96.5% pure.

Structural characterization of 9-arylimino noscapinoids, 4-6

(S)-3-((R)-9-((E)-((5-bromothiophen-2-yl) methylene)amino)-4-methoxy-6-methyl-5,6,7,8-tetrahydro-[1,3]dioxolo[4,5-g] isoquinolin-5-yl)-6,7dimethoxyisobenzofuran-1(3H)-one (4)

Yield: 82%. Nature: White solid. Mp. 94-96°C. IR (KBr): 3448, 2929, 1758, 1623, 1497, 1424, 1381, 1267, 1209, 1121, 1035, 970, 887, 795, 736, 696, 501 cm^{-1}. ^{1}H NMR (500 MHz, $CDCl_3$): δ 8.88 (s, 1H, N=CH), 7.14 (d, J = 3.8 Hz, 1H, Ar-H), 7.07 (d, J = 3.8 Hz, 1H, Ar-H), 7.01 (d, J = 8.2 Hz, 1H, Ar-H), 6.36 (d, J = 8.2 Hz, 1H, Ar-H), 5.98 (dd, J = 1.3, 16.0 Hz, 2H,

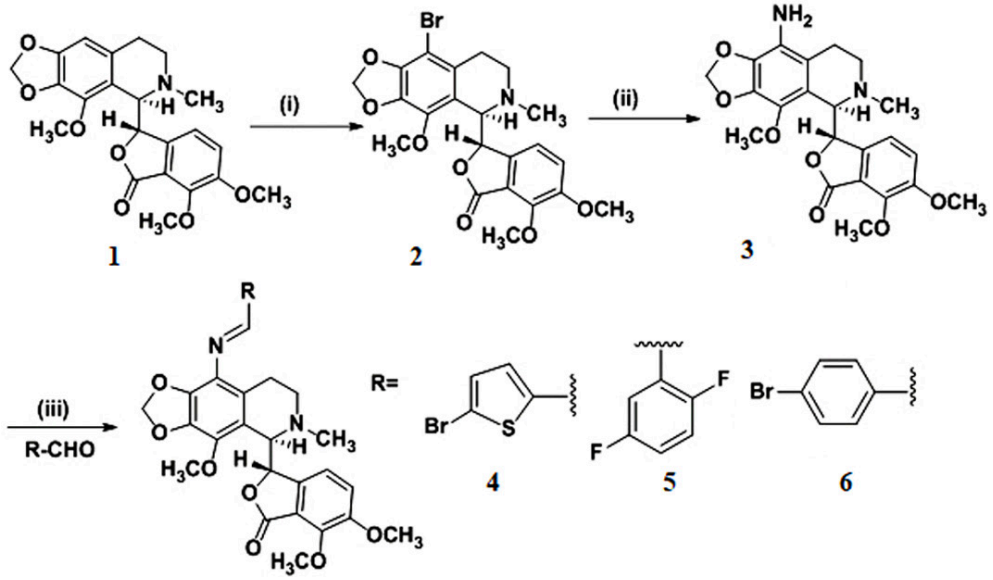

Figure 3. General chemical reaction for chemical synthesis of 9-arylimino noscapinoids 4-6, rationally design in the study. Reaction conditions: (i) 48% HBr, Br_2-water, rt, 2h (ii) CuI, NaN_3, L-Proline, DMF, 140°C, 4h, (iii) RCHO, EtOH, Reflux, 24h

O-C*H*2-O), 5.55 (d, *J* = 4.5 Hz, 1H, Ar-CH, (C3-phthalide)), 4.36 (d, *J* = 4.5 Hz, 1H, Ar-CH, (C5'-isoquinoline)), 4.10 (s, 3H, -OCH3), 4.02 (s, 3H, -OCH3), 3.86 (s, 3H, -OCH3), 2.98-2.91 (m, 1H, -C*H*H-*N*-CH3 (C7'-isoquinoline)), 2.75-2.69 (m, 1H, -CH*H*-*N*-CH3 (C7'-isoquinoline)), 2.53 (s, 3H, *N*-C*H*3), 2.44-2.38 (m, 1H, Ar-C*H*H (C8'- isoquinoline)), 2.08-2.01 (m, 1H, Ar-CH*H* (C8'- isoquinoline)). ^{13}C NMR (100 MHz, CDCl3): δ 168.0, 152.0, 147.4, 145.5, 140.7, 137.1, 135.3, 134.8, 129.4, 125.3, 122.9, 120.9, 119.9, 117.9, 117.7, 110.8, 100.6, 81.7, 62.1, 60.7, 59.6, 56.7, 49.1, 45.9, 22.3. MS (ESI-MS) *m/z*: 603 [M+H]+ HRMS (ESI): Calcd for $C_{27}H_{26}BrN_2O_7S$[M+H]+: 603.06116, found: 603.06173.

(S)-3-((R)-9-((E)-(2,5-difluorobenzylidene) amino)-4-methoxy-6-methyl-5,6,7,8 tetrahydro-[1,3]dioxolo[4,5-g]isoquinolin-5-yl)-6,7-dimethoxyisobenzofuran-1(3H)-one (5) Yield: 74%. Nature: White solid. mp: 145-147°C. IR (KBr): 33571, 2944, 2793, 1762, 1628, 1491, 1428, 1387, 1272, 1142, 1043, 965, 813, 725 cm^{-1}. ^{1}H NMR (400 MHz, $CDCl_3$): δ 9.13 (d, *J*= 2.4 Hz, 1H, N=CH), 7.87-7.81 (m, 1H, Ar-H), 7.14-7.07 (m, 2H, Ar-H), 7.00 (d, *J* = 8.3 Hz, 1H, Ar-H), 6.33 (d, *J* = 8.3 Hz, 1H, Ar-H), 6.02 (dd, *J* = 1.3, 15.6 Hz, 2H, O-C*H*2-O), 5.57 (d, *J* = 4.4 Hz, 1H, Ar-CH, (C3-phthalide)), 4.39 (d, *J* = 4.4 Hz, 1H, Ar-CH, (C5'-isoquinoline)), 4.10 (s, 3H, -OCH3), 4.04 (s, 3H, -OCH3), 3.86 (s, 3H, -OCH3), 3.05-2.95 (m, 1H, -C*H*H-*N*-CH3 (C7'-isoquinoline)), 2.77-2.69 (m, 1H, -CH*H*-*N*-CH3 (C7'-isoquinoline)), 2.55 (s, 3H, *N*C*H*3), 2.46-2.37 (m, 1H, Ar-C*H*H (C8'-isoquinoline)), 2.11-2.00 (m, 1H, Ar-CH*H* (C8'-isoquinoline)). ^{13}C NMR (125 MHz, $CDCl_3$): δ 168.0, 159.8 (d, *J*C-F = 31.7 Hz), 157.9(d, *J*C-F= 38.1 Hz), 153.2, 152.1, 147.6, 141.3, 139.47, 139.43, 134.4, 129.8, 126.1 (dd, *J*C-F = 8.1, 11.8 Hz), 124.9, 119.8, 119.1 (dd, *J*C-F = 9.0, 25.4 Hz), 117.8, 117.6, 117.1 (dd, *J*C-F = 8.1, 23.6 Hz), 112.9 (dd, *J*C-F = 2.7, 25.4 Hz), 101.1, 81.7, 62.2, 60.8, 59.5, 56.7, 49.3, 45.8, 22.8. MS (ESI-MS) *m/z*: 553 [M+H]+ HRMS (ESI): Calcd for $C_{29}H_{27}F_2N_2O_7$ [M+H]+: 553.17808, found: 553.17669.

(S)-3-((R)-9-((E)-(4-bromobenzylidene) amino)-4-methoxy-6-methyl-5,6,7,8-tetrahydro-[1,3]dioxolo[4,5-g]isoquinolin-5-yl)-6,7-dimethoxyisobenzofuran-1(3H)-one (6) Yield: 76%. Nature: White solid. mp: 93-95°C. IR (KBr): 3449, 2936, 2795, 1758, 1626, 1494, 1383, 1267, 1124, 1034, 970, 821 cm-1. ^{1}H NMR (500 MHz, $CDCl_3$): δ 8.84 (s, 1H, N=CH), 7.76 (d, *J* = 8.5 Hz, 2H, Ar-H), 7.58 (d, *J* = 8.5 Hz, 2H, Ar-H), 6.99 (d, *J* = 8.3 Hz, 1H, Ar-H), 6.34 (d, *J* = 8.3 Hz, 1H, Ar-H), 5.99 (dd, *J* = 1.3, 14.9 Hz, 2H, O-C*H*2-O), 5.57 (d, *J* = 4.4 Hz, 1H, Ar-CH, (C3-phthalide)), 4.38 (d, *J* = 4.4 Hz, 1H, Ar-CH, (C5'-isoquinoline)), 4.10 (s, 3H, -OCH3), 4.03 (s, 3H, -OCH3), 3.85 (s, 3H, -OCH3), 3.04-2.93 (m, 1H, -C*H*H-*N*-CH3 (C7'-isoquinoline)), 2.75-2.68 (m, 1H, -CH*H*-*N*-CH3 (C7'-isoquinoline)), 2.54 (s, 3H, *N*C*H*3), 2.46-2.37 (m, 1H, Ar-C*H*H (C8'-isoquinoline)), 2.10-2.00 (m, 1H, Ar-CH*H* (C8'-isoquinoline)). ^{13}C NMR (100 MHz, CDCl3): δ 168.1, 160.1, 152.1, 147.6, 141.4, 139.2, 139.0, 135.9, 134.5, 131.8, 129.6, 129.3, 125.4, 125.2, 119.8, 118.3, 117.8, 117.6, 100.9, 81.7, 62.2, 60.9, 59.5, 56.7, 49.3, 45.8, 22.7. MS (ESI-MS) *m/z*: 595 [M+H]+ HRMS (ESI): Calcd for $C_{29}H_{28}BrN_2O_7$ [M+H]+: 595.10744, found: 595.10635.

Cell culture and reagents

The human breast cancer cell lines, MCF-7 and MDA-MB-231 were acquired from the Institute of Life Science, Bhubaneswar, India. The normal human embryonic kidney cell (293T) (passage number 12) was obtained from Dr. S.K. Singh, King George's Medical University, Lucknow, India. Stock solution (100 mM) of 9-arylimino noscapinoids, 4-6 were prepared with 1% dimethyl sulfoxide (DMSO). The cells were grown in a 5% CO_2 and 95% humidity in Dulbecco's modified Eagle medium (DMEM) at a temperature of 37°C, supplemented with 10 % fetal bovine serum (FBS) and antibiotics. Cells with a 70-80 % confluence were subcultured for bioassays using trypsin-EDTA (0.25 %).

Cellular proliferation assay

The cell proliferation assay was performed using two human breast cancer cell lines MCF-

7 and MDA-MB-231 as well as a normal human embryonic kidney cell (293T) as described previously [16]. Briefly, the cells were seeded at a density of $5x10^3$ cells per well in 96-well plates. The cells were treated with 5 to 100 µM of noscapine and 9-arylimino noscapinoids, 4-6. After 72h of treatment, the viability of the cell was checked by sulforhodamine B assay. The plate was read at a wavelength of 564 nm using a SPECTRAmax PLUS 384 microplate spectrophotometer. Fifty percent inhibitory concentration (IC_{50}) of molecules was determined using the online tool Quest GraphTM IC_{50} Calculator (AAT Bioquest, Inc., Sunnyvale, CA, USA, https://www.aatbio.com/tools/ic50-calculator).

Cell cycle progression assay

The progression in the mitotic cell cycle with the treatment of 9-arylimino noscapinoids, 4-6 was performed as reported earlier [23]. Briefly, MDA-MB-231 cells were seeded at a density of $1x10^5$ in a 6-well culture plate overnight and were treated with IC_{50} concentration of noscapine (51.6 µM) and 9-arylimino noscapinoids, 4-6 (32.6, 15.4 and 7.7 µM respectively). After 72 h of treatment, cells were analyzed using flow cytometry (BD FACS Aria-III) to estimate the percentage of cells in the different stages of the cell cycle.

Apoptosis assay

Induction of apoptosis was performed as described earlier [23]. The breast cancer cells, MDA-MB-231 ($3x10^4$) were seeded on 12 well culture plate and incubated for 24 h with a complete medium. The cells were treated with IC_{50} concentration of noscapine (51.6 µM) and 9-arylimino noscapinoids, 4-6 (32.6, 15.4 and 7.7 µM respectively) and were harvested at 72 h. The apoptotic cells were detected by using an apoptosis detection kit based on the instruction provided by the manufacture (Sigma-Aldrich, USA) using flow cytometry (BD FACS Aria-III). Viable cells (Annexin V^- / PI^-), early apoptotic cells (Annexin V^+ / PI^-), late apoptotic/necrotic cells (Annexin V^+ / PI^+) and late necrotic cells (Annexin V^- / PI^+) were identified and determined their percentage.

Extraction and purification of tubulin

Microtubule from the goat brain was isolated by two cycles of temperature- and GTP-dependent polymerization and depolymerization [24]. It was then purified by phosphocellulose chromatography as reported earlier [25] and the amount of purified tubulin was estimated using the Bradford method [26]. Aliquots were frozen in liquid nitrogen and preserved at -80°C until used.

Tryptophan quenching assay

A fluorescence quenching assay was performed to determine the binding of a chemical onto tubulin [27]. It is because tubulin is autofluorescence in nature due to the presence of several tryptophan amino acids and it was reduced when a molecule binds on it. Tubulin (2 µM) was treated with 9-arylimino noscapinoids 4-6 at a concentration of 25 µM in PEM buffer (50 mM pipes, 3 mM $MgSO_4$, 1 mM EGTA, pH 6.8) in a water bath (35°C; 45 min). They were then excited at 295 nm and the emission reading at 310-400 nm was obtained. A FlouroMax® 4 spectrofluorometer (Horiba Scientifc, Edison, NJ) supported by FluorEssence 3.5 software was used for the spectrofluorimetric titrations.

Results and discussion

Many derivatives of noscapine have been developed to increase its therapeutic outcome [8,11,27,28-30]. These derivatives were demonstrated to bind tubulin, perturb cell-cycle progression, inhibit cell proliferation and induce apoptosis in a variety of cancer cells of different tissue origin [31]. The derivatives generated by modification of the C-9 position on the isoquinoline ring system of noscapine were shown to possess superior activity [28,32]. Based upon this momentum, we have rationally designed a new series of derivatives of noscapine by substituting arylimino groups (Schiff bases) at C-9 position to examine their anticancer potential.

Molecular dynamics simulation

The library composed of 9-arylimino derivatives of noscapine was docked onto αβ-tubulin heterodimer and ranked according to docking

score. The top ranked three noscapinoids 4-6 (Fig. 2) having lowest docking scores ranging from -4.219 to -5.135 kcal/mol in comparison to noscapine (-3.586 kcal/mol) (Table 1) were selected. The αβ-tubulin heterodimer bound to molecules 4-6 were MD simulated for 100 ns. The system's stability during the period of the simulation was monitored by the root means square deviations (RMSD) of Cα-carbons (supplementary information S14). The deviations in the RMSD plot were very small after equilibration and were found to be stable after 20 ns of simulation. Similarly, the root mean square fluctuations (RMSF) of amino acids in the bound form with ligands and in the free form were not so much different (within the range of 1 to 2.5 Å) indicating that the residues were more rigid (supplementary information S15). The top 5 complex structures of tubulin and 9-arylimino noscapinoids, 4-6 having the lowest total energy from the MD trajectory were used to generate the average structure to elucidate their binding mode. All the three 9-arylimino noscapinoids accommodated well inside the noscapinoids binding pocket (Fig. 4) between α- and β- tubulin interface. Their interactions with the binding site amino acids are shown in the ligplot (Fig. 5). The 9-arylimino noscapinoid, 6 binds with 2 hydrogen bonds (represented by a dashed line and the number indicated the bond length) (Fig. 5c). In contrast, the 9-arylimino noscapinoids, 4 and 5 revealed only 1 hydrogen bond with the binding site residues (Fig. 5a,b). Besides, hydrogen bonding, a good number of hydrophobic interactions were involved in the binding of 9-arylimino noscapinoids 4-6 with

Table 1a. Docking score, free energy of binding and its components (kcal/mol) for the 9-arylimino noscapinoids with αβ tubulin dimer using MM-PBSA method

Energy components (kcal/mol)	Noscapine	4	5	6
Glide XP_{score}	-3.856	-4.219	-4.367	-5.135
ΔE_{ele}	-319.2	-326.5	-338.4	-344.3
ΔE_{vdw}	-65.36	-73.62	-77.27	-79.37
ΔE_{gas}	-383.4	-389.7	-396.2	-409.3
$\Delta G_{sol\text{-}np}$	-7.254	-8.128	-8.927	-9.154
ΔG_{PB}	354.7	359.5	365.2	372.4
$\Delta G_{solv,PB}$	348.3	357.2	362.4	368.2
$\Delta G_{ele,PB}$	33.74	41.43	46.31	48.19
$\Delta G_{bind,PB}$	-34.47	-37.24	-39.73	-43.62

Table 1b. Free energy of binding and its components (kcal/mol) for the 9-arylimino noscapinoids with αβ tubulin dimer using MM-GBSA method

Energy components (kcal/mol)	Noscapine	4	5	6
ΔE_{ele}	-319.2	-326.5	-338.4	-344.3
ΔE_{vdw}	-65.36	-73.62	-77.27	-79.37
ΔE_{gas}	-383.4	-389.7	-396.2	-409.3
$\Delta G_{sol\text{-}np}$	-7.254	-8.128	-8.927	-9.154
ΔG_{GB}	349.4	351.3	347.5	364.3
$\Delta G_{solv,GB}$	341.7	344.6	347.4	358.7
$\Delta G_{ele,GB}$	28.95	32.74	34.73	36.44
$\Delta G_{bind,GB}$	-40.27	-45.41	-47.74	-49.72

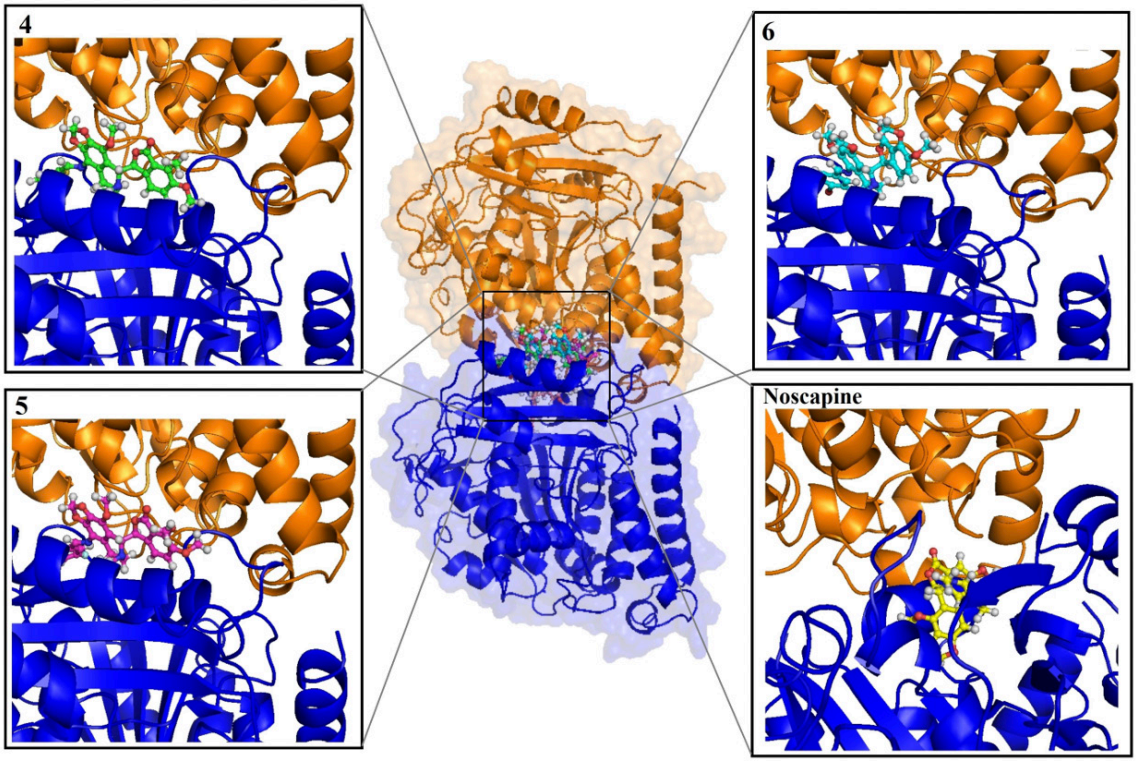

Figure 4. The newly designed 9-arylimino noscapinoids 4-6 are accomodated well inside the binding site at the interface of α- and β- tubulin. α-tubulin is represented in blue colour and β-tubulin is represented in brown colour

binding site residues (Supplementary Table S16-S19).

Theoretical binding affinity calculation

The binding affinity of all the three 9-arylimino noscapinoids 4-6 was calculated using MM-PBSA and MM-GBSA methods. All three noscapinoids displayed stable interaction throughout the simulation. Among them, the 9-arylimino noscapinoid 6 showed the best binding affinity with the predicted free energy of binding ($\Delta G_{bind,pred}$) of -49.72 kcal/mol followed by 5 with -47.74 kcal/mol and 4 with -45.41 kcal/mol using the MM-PBSA method (Table 1). Using the MM-GBSA method also, 9-arylimino noscapinoid 6 showed the highest binding affinity with the value of -43.62 kcal/mol followed by 5 with -39.73 kcal/mol and 4 with -37.24 kcal/mol (Table 1). Overall, all the three 9-arylimino noscapinoids 4-6 revealed better binding affinity compared to noscapine (-34.47 kcal/mol and -40.27 kcal/mol) respectively using both MM-GBSA and MM-PBSA (Table 1). This could be attributed to the formation of both hydrogen bonds and hydrophobic interaction of 9-arylimino noscapinoids with surrounding amino acids in the binding pocket. A similar study has been performed earlier for designing novel derivatives of noscapine based on a combination approach of molecular docking and MD simulation. A panel of three different 9-arylimino noscapinoids has been designed *in silico*. These noscapinoids were predicted to have a better binding affinity with tubulin based on molecular docking and LIE-SGB predicted binding energy [33]. In contrast, the three new 9-arylimino derivatives of noscapine screened out in this study from the library were predicted to have better binding affinity compared to the previously reported 9-arylimino noscapinoids. A combination of MD simulation and MM-PBSA method has been used earlier to identify potential inhibitors against targeted proteins [34,35].

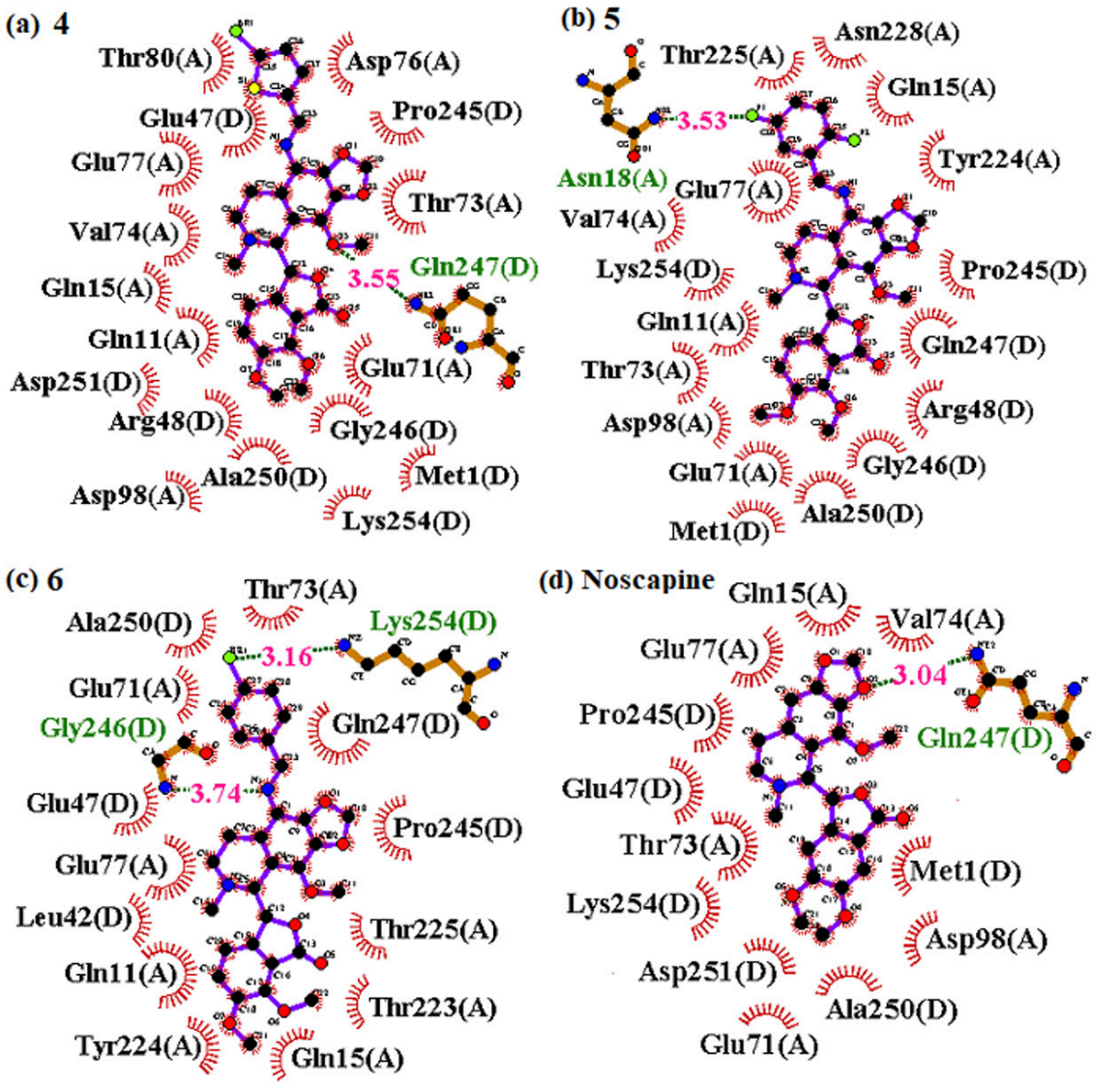

Figure 5. The ligplot analysis showed the interaction of binding site amino acids with the 9-arylimino noscapinoids 4-6 and noscapine. The binding site residues involved in the interactions are slightly different mainly because of the variation in functional groups. The hydrogen bonds formed (if any) are represented as dotted lines

Arylimino noscapinoids, 4-6 inhibits proliferation of MCF-7 and MDA-MB-231

The 9-arylimino noscapinoids, 4-6 inhibited proliferation of MCF-7 and MDA-MB-231 cells in a dose-dependent manner (supplementary information S20). The 9-arylimino derivatives of noscapine, 4-6 revealed promising anti-proliferative activity compared to noscapine. The IC_{50} value was 45.2 µM, 26.8 µM, 11.6 µM and 3.0 µM for noscapine, 4, 5 and 6, respectively for MCF-7 cells (Table 2). In contrast, IC_{50} value of 51.6 µM, 32.6 µM, 15.4 µM and 7.7 µM was measured for noscapine, 4, 5 and 6, respectively for MDA-MB-231 cells. The differences in IC_{50} values obtained using MCF-7 (a triple positive for receptor proteins) and MDA-MB-231 (a triple negative for receptor proteins) cell lines revealed that the anti-proliferative activity for these 9-arylimino noscapinoids were cell-type dependent. Further, the toxicity if any to the normal healthy cells with the treatment of noscapine and its 9-arylimino derivatives, 4-6

Table 2. IC_{50} values of designed 9-arylimino noscapinoids, 4-6 using two human breast cancer cell lines MCF-7 and MDA-MB-231 and a normal human embryonic kidney cells (293T) The molecules screened out 4-6 have better anti-proliferative activity compared to noscapine without any significant toxicity to normal healthy cells

	IC_{50} (μM)			
	Noscapine	4	5	6
MCF-7	45.2±4.3	26.8±2.6	11.6±1.6	3.0±0.9
MDA-MB-231	51.6±4.7	32.6±3.2	15.4±1.9	7.7±1.3
293T normal cell	212.5±2.7	172.1±4.6	167.4±3.9	152.5±4.8

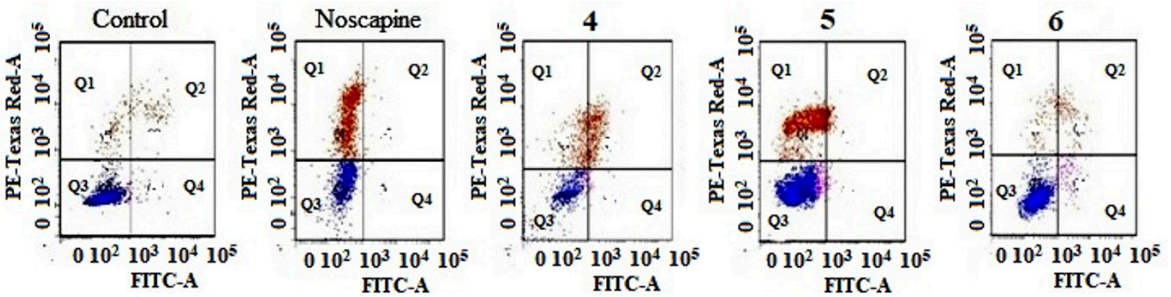

Figure 6. Analysis of apoptosis to MDA-MB-231 cells treated with noscapine and 9-arylimino noscapinoids, 4-6 based on flow cytometry analysis. The cells were treated with IC_{50} concentration for 72 hours and compared with non-treated control cells. Annexin-V in combination with propidium iodide (PI) were used to distinguish among 3 sub-populations of cells: PI- and AnnexinV- cells indicates viable cells (Q3), PI- and Annexin V+ cells indicates early apoptotic cells (Q1), whereas PI+ and Annexin V+ cells indicates late apoptotic cells (Q2)

was determined using normal human embryonic kidney cells (293T). It was found that noscapine and its 9-arylimino derivatives, 4-6 revealed < 5% cell killing to normal cells even at a high concentration of 100 μM (supplementary information 21), indicating that the molecules are not affecting the normal cells and only selectively inhibiting the proliferation of cancer cells. In contrast, the 9-arylimino derivatives of noscapine, 4-6 at relatively low concentrations (5.0 μM) significantly stimulated proliferation of 293T cells, while at higher concentrations (100 μM) inhibited proliferation of 293T cells (< 5%).

9-Arylimino noscapinoids, 4-6 induced apoptosis to cancer cells

The apoptotic cells were easily quantified using FACS analysis using fluorescent dyes, Annexin V and propidium iodide. The percentage of early apoptotic and late apoptotic cells using MDA-MB-231 cell lines for the treatment of noscapine and 9-arylimino noscapinoids, 4-6 with IC_{50} concentration for 72 h were collated in Table III. A representative figure of flow cytometry analysis is shown in Fig. 6. After 72 h, the control untreated cells contained only very few early apoptotic (2.3%) and late apoptotic cells (1.2%), which were considered as the background cell death due to regular trauma during cell culture (Table 3). In contrast, the percentage of early apoptotic cells of 14%, 18%, 55%, and 20%; late apoptotic cells of 31%, 40%, 12% and 20% as well as necrotic cells of 1.1%, 2.3%, 3.4% and 20% with treatments of noscapine and its 9-arylimino noscapinoids, 4-6, respectively were found to be significantly high compared to untreated cells (Table 3).

Inhibition of cell cycle progression

The inhibition in cell cycle progression with the treatment of noscapine and 9-arylimino

Table 3. Quantification of viable (Q3), early apoptotic (Q1), late apoptotic (Q2) and necrotic (Q4) cells after treatment with noscapine and 9-arylimino noscapinoids, 4-6 by flow cytometry

Viability/Apoptotic	Untreated	Noscapine	4	5	6
Q1	2.3%	14%	18%	55%	20%
Q2	1.2%	31%	40%	12%	20%
Q3	93%	49%	40%	37%	24%
Q4	0.5%	1.1%	2.3%	3.4%	20%

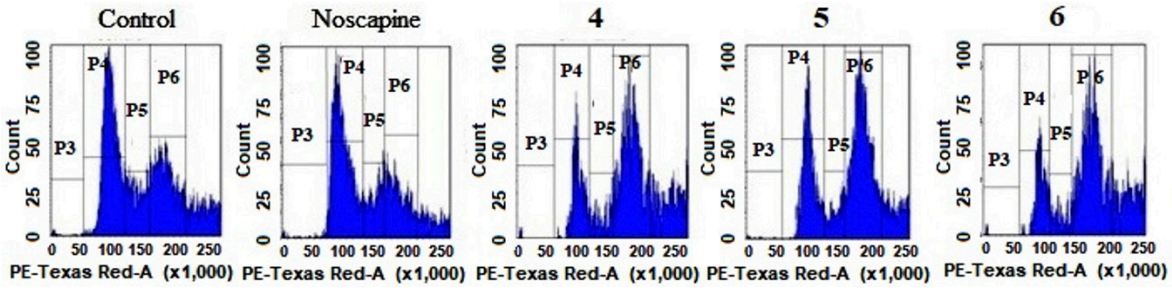

Figure 7. A representative figure of cell cycle distribution as determined by flow cytometry in MDA-MB-231 cells treated with IC_{50} concentration of Noscapine and its 9-arylimino derivatives 4-6. The test compounds inhibit cell cycle progression at mitosis followed by the appearance of a characteristic hypodiploid (sub-G1) DNA peak, indicative of apoptosis. P3: sub-G1 phase, P4: G1 phase, P5: S-phase and P6: G2/M phase

Table 4. Effect of noscapine and its 9-arylimino noscapinoids, 4-6 on cell cycle profile of MDAMB-231 cells treated with IC_{50} concentration for 72 hour

	72 hours			
	Sub-G_1	G_0/G_1	S	G_2/M
Control	0.7	20	22.4	7.2
Noscapine	4.9	17.5	15.1	15.5
4	7.5	13.8	10	28.1
5	8.9	14	8.2	34.7
6	10.8	25	10.0	39.7

noscapinoids, 4-6 at IC_{50} concentration using MDA-MB-231 is represented in Fig. 7. The amount of DNA accumulated in a cell with the treatment of noscapinoids is detected by the fluorescence dye, propidium iodide using flow cytometer. The cells with 2N DNA are in the G1 phase while with 4N DNA are in G2 and M phases. DNA content in between 2N and 4N peaks represents, the cells are in the S phase. In contrast, less than 2N DNA indicates the apoptotic cells in which the DNA is degraded to different extents. Treatment of MDA-MB-231 cells with the 9-arylimino derivatives, 4-6 led to inhibition of cell cycle progression in the G2/M phase. There was a high accumulation of cells in the G2/M phase compared to untreated cells (Table 4). In contrast to the G2/M block, a characteristic hypodiploid DNA content peak (sub-G1) was seen to rise at 72 h of treatment, indicating dying cells.

Tubulin binding assay

Intrinsic fluorescence of tubulin is primarily due to the presence of aromatic amino acid, tryptophan. It is measured by exciting at 295 nm. The decreased fluorescence intensity in the presence of 9-arylimino noscapinoids, 4-6 suggests the binding of these compounds to tubulin. The relative percentage of decrease in fluorescence intensity was 10.92%, 16.42%, 23.28% and 31.64% in presence of 25 µM of noscapine and its 9-arylimino noscapinoids, 4-6 respectively (Fig. 8), compared to control. These 9-arylimino noscapinoids revealed increased

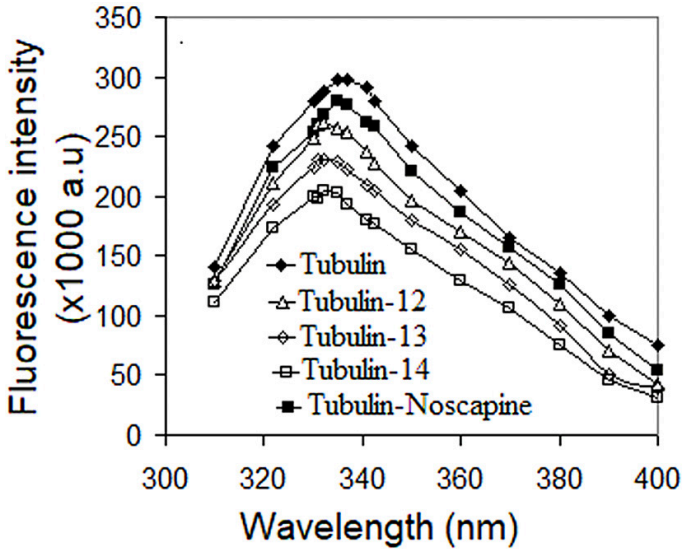

Figure 8. Treatment of Noscapine and its 9-arylimino derivatives, 4-6 with purified tubulin showed quenching of the intrinsic tubulin fluorescence emission intensity to different extents, indicating binding of these noscapinoids to tubulin

binding affinity with tubulin compared to noscapine.

Conclusion

In conclusion, a new series of derivatives of noscapine, 9-imine-noscapinoids was developed in a quest of accelerating its anticancer activity. This series of noscapine derivatives were developed by substitution of arylimino groups at C-9 position of noscapine scaffold by *in silico* combinatorial approach. Through *in silico* screening, three top ranked molecules were finally screened out for chemical synthesis and experimental evaluation of anticancer activity. These 9-arylimino noscapinoids, 4-6 have shown improved anti-proliferative activity to breast cancer cells compared to noscapine. Therefore, these derivatives may prove efficacious not only in the treatment of breast cancer but also for other types of cancers. Our results compel us to continue to examine the effects of these novel compounds on *in vivo* animal experiments with the final goal of taking it to the human clinical study.

Acknowledgement

We would like to acknowledge the financial support provided by the ICMR (Grant No. 5/13/11/2020-NCD-III), Government of India. We are grateful to Dr. Manu Lopus and UM-DAE Centre for Excellence in Basic Sciences for providing extended facilities.

References

1. **Kavanagh, J.J. and Kudelka, A.P. (1993).** Systemic therapy for gynecologic cancer. Current Opinion in Oncology. 5(5): 891-899.
2. **Rowinsky, E.K. and Donehower, R.C. (1991).** The clinical pharmacology and use of antimicrotubule agents in cancer chemotherapeutics. Pharmacology & Therapeutics. 52(1): 35-84.
3. **Ye, K., Ke, Y., Keshava, N., Shanks, J., Kapp, J.A., Tekmal, R.R., Petros, J. and Joshi, H.C. (1998).** Opium alkaloid noscapine is an antitumor agent that arrests metaphase and induces apoptosis in dividing cells. Proceedings of the National Academy of Sciences. 95(4): 1601-1606.
4. **Landen, J.W., Lang, R., McMahon, S.J., Rusan, N.M., Yvon, A.M., Adams, A.W., Sorcinelli, M.D., Campbell, R., Bonaccorsi, P., Ansel, J.C., Archer, D.R., Wadsworth, P., Armstrong, C.A. and Joshi, H.C. (2002).** Noscapine alters

microtubule dynamics in living cells and inhibits the progression of melanoma. Cancer Research. 62(14): 4109-4114.

5. **Karlsson, M.O., Dahlström, B., Eckernäs, S.A., Johansson, M. and Alm, A.T. (1990).** Pharmacokinetics of oral noscapine. European Journal of Clinical Pharmacology. 39(3): 275-279.
6. **Manchukonda, N.K., Sridhar, B., Naik, P.K., Joshi, H.C., and Kantevari, S. (2012).** Copper (I) mediated facile synthesis of potent tubulin polymerization inhibitor, 9-amino-α-noscapine from natural α-noscapine. Bioorganic & Medicinal Chemistry Letters. 22(8): 2983-2987.
7. **Manchukonda, N.K., Naik, P.K., Santoshi, S., Lopus, M., Joseph, S., Sridhar, B. and Kantevari, S. (2013).** Rational design, synthesis, and biological evaluation of third generation α-noscapine analogues as potent tubulin binding anti-cancer agents. PloS One. 8(10): e77970.
8. **Santoshi, S., Manchukonda, N.K., Suri, C., Sharma, M., Sridhar, B., Joseph, S., Lopus, M., Kantevari, S., Baitharu, I. and Naik, P.K. (2015**). Rational design of biaryl pharmacophore inserted noscapine derivatives as potent tubulin binding anticancer agents. Journal of Computer-Aided Molecular Design. 29(3): 249-270.
9. **Oliva, M.A., Prota, A.E., Rodríguez-Salarichs, J., Bennani, Y.L., Jiménez-Barbero, J., Bargsten, K., Canales, Á., Steinmetz, M.O. and Díaz, J.F. (2020)**. Structural Basis of Noscapine Activation for Tubulin Binding. Journal of Medicinal Chemistry. 63(15): 8495-8501.
10. **Ali, I., Haque, A., Saleem, K. and Hsieh, M.F. (2013).** Curcumin-I Knoevenagel's condensates and their Schiff's bases as anticancer agents: synthesis, pharmacological and simulation studies. Bioorganic & Medicinal Chemistry. 21(13): 3808-3820.
11. **Sondhi, S.M., Arya, S., Rani, R., Kumar, N. and Roy, P. (2012).** Synthesis, anti-inflammatory and anticancer activity evaluation of some mono-and bis-Schiff's bases. Medicinal Chemistry Research. 21(11): 3620-3628.
12. **Gordon, M.S., Binkley, J.S., Pople, J.A., Pietro, W.J. and Hehre, W.J. (1982).** Self-consistent molecular-orbital methods. 22. Small split-valence basis sets for second-row elements. Journal of the American Chemical Society. 104(10): 2797-2803.
13. **Beck, A.D. (1993).** Density-functional thermochemistry. III. The role of exact exchange. J. Chem. Phys. 98(7): 5648-6.
14. **Dash, S.G., Kantevari, S. and Naik, P.K. (2021).** Combination Regimen of Amino-Noscapine and Docetaxel for Evaluation of Anticancer Activity. Analytical Chemistry Letters. 11(2): 215-229.
15. **Halgren, T.A., Murphy, R.B., Friesner, R.A., Beard, H.S., Frye, L.L., Pollard, W.T. and Banks, J.L. (2004).** Glide: a new approach for rapid, accurate docking and scoring. 2. Enrichment factors in database screening. Journal of Medicinal Chemistry. 47(7): 1750-1759.
16. **Meher, R.K., Nagireddy, P.K.R., Pragyandipta, P., Kantevari, S., Singh, S.K., Kumar, V. and Naik, P.K. (2021).** In silico design of novel tubulin binding 9-arylimino derivatives of noscapine, their chemical synthesis and cellular activity as potent anticancer agents against breast cancer. Journal of Biomolecular Structure and Dynamics. 1-12.
17. **Kollman, P.A., Massova, I., Reyes, C., Kuhn, B., Huo, S., Chong, L. and Cheatham, T.E. (2000).** Calculating structures and free energies of complex molecules: combining molecular mechanics and continuum models. Accounts of Chemical Research. 33(12): 889-897.
18. **Massova, I., and Kollman, P.A. (2000).** Combined molecular mechanical and continuum solvent approach (MM-PBSA/GBSA) to predict ligand binding. Perspectives in Drug Discovery and Design. 18(1): 113-135.
19. **Weis, A., Katebzadeh, K., Söderhjelm, P., Nilsson, I. and Ryde, U. (2006).** Ligand affinities predicted with the MM/PBSA method: dependence on the simulation

method and the force field. Journal of Medicinal Chemistry. 49(22): 6596-6606.

20. **Xu, L., Sun, H., Li, Y., Wang, J. and Hou, T. (2013).** Assessing the performance of MM/PBSA and MM/GBSA methods. 3. The impact of force fields and ligand charge models. The Journal of Physical Chemistry B. 117(28): 8408-8421.
21. **Hou, T., Wang, J., Li, Y. and Wang, W. (2011).** Assessing the performance of the molecular mechanics/Poisson Boltzmann surface area and molecular mechanics/ generalized Born surface area methods. II. The accuracy of ranking poses generated from docking. Journal of Computational Chemistry. 32(5): 866-877.
22. **Sun, H., Li, Y., Shen, M., Tian, S., Xu, L., Pan, P., Guan, Y., and Hou, T. (2014).** Assessing the performance of MM/PBSA and MM/GBSA methods. 5. Improved docking performance using high solute dielectric constant MM/GBSA and MM/PBSA rescoring. Physical Chemistry Chemical Physics: PCCP. 16(40): 22035-22045.
23. **Patel, A.K., Meher, R.K., Nagireddy, P.K., Pedapati, R.K., Pragyandipta, P., Kantevari, S., Naik, M.R. and Naik, P.K. (2021).** Rational design, chemical synthesis and cellular evaluation of novel 1,3-diynyl derivatives of noscapine as potent tubulin binding anticancer agents. Journal of Molecular Graphics and Modelling. 106: 107933
24. **Hamel, E. and Lin, C.M. (1981).** Glutamate-induced polymerization of tubulin: characteristics of the reaction and application to the large-scale purification of tubulin. Archives of Biochemistry and Biophysics. 209(1): 29-40.
25. **Panda, D., Chakrabarti, G., Hudson, J., Pigg, K., Miller, H.P., Wilson, L. and Himes, R.H. (2000).** Suppression of microtubule dynamic instability and treadmilling by deuterium oxide. Biochemistry. 39(17): 5075-5081.
26. **Bradford, M.M. (1976).** A rapid and sensitive method for the quantitation of microgram quantities of protein utilizing the principle of protein-dye binding. Analytical Biochemistry. 72(1-2): 248-254.
27. **Dash, S.G., Suri, C., Nagireddy, P.K.R., Kantevari, S. and Naik, P.K. (2020).** Rational design of 9-vinyl-phenyl noscapine as potent tubulin binding anticancer agent and evaluation of the effects of its combination on Docetaxel. Journal of Biomolecular Structure and Dynamics. 1-14.
28. **Aneja, R., Vangapandu, S.N., Lopus, M., Chandra, R., Panda, D. and Joshi, H.C. (2006a).** Development of a novel nitro-derivative of noscapine for the potential treatment of drug-resistant ovarian cancer and T-cell lymphoma. Molecular Pharmacology. 69(6): 1801-1809.
29. **Aneja, R., Lopus, M., Zhou, J., Vangapandu, S.N., Ghaleb, A., Yao, J. and Joshi, H.C. (2006b).** Rational Design of the Microtubule-Targeting Anti-Breast Cancer Drug EM015. Cancer Research. 66(7): 3782-3791.
30. **Aneja, R., Vangapandu, S.N. and Joshi, H.C. (2006c).** Synthesis and biological evaluation of a cyclic ether fluorinated noscapine analog. Bioorganic & Medicinal Chemistry. 14(24): 8352-8358.
31. **Manchukonda, N.K., Naik, P.K., Sridhar, B. and Kantevari, S. (2014).** Synthesis and biological evaluation of novel biaryl type α-noscapine congeners. Bioorganic & Medicinal Chemistry Letters. 24(24): 5752-5757.
32. **Aneja, R., Vangapandu, S.N., Lopus, M., Viswesarappa, V.G., Dhiman, N., Verma, A., Chandra, R., Panda, D. and Joshi, H.C. (2006a).** Synthesis of microtubule-interfering halogenated noscapine analogs that perturb mitosis in cancer cells followed by cell death. Biochemical Pharmacology. 72(4): 415-426.
33. **Patel, A.K., Meher, R.K., Nagireddy, P.K., Pragyandipta, P., Pedapati, R.K., Kantevari, S. and Naik, P.K. (2021).** 9-Arylimino noscapinoids as potent tubulin binding anticancer agent: chemical synthesis and cellular evaluation against breast tumour cells. SAR and QSAR in Environmental

Research. 32(4): 269-291.

34. **Bhardwaj, V.K., Singh, R., Sharma, J., Das, P. and Purohit, R. (2020).** Structural based study to identify new potential inhibitors for dual specificity tyrosine-phosphorylation- regulated kinase. Computer Methods and Programs in Biomedicine. 194: 105494.
35. **Bhardwaj, V.K. and Purohit, R. (2021).** Targeting the protein-protein interface pocket of Aurora-A-TPX2 complex: rational drug design and validation. Journal of Biomolecular Structure & Dynamics. 39(11): 3882-3891.